Design and Fabrication of Pellets for Magnesium Production by Carbothermal Reduction

BORIS A. CHUBUKOV, AARON W. PALUMBO, SCOTT C. ROWE, MARK A. WALLACE, KEVIN Y. SUN, and ALAN W. WEIMER

For carbothermal reduction (CTR) to be an economic and clean process for magnesium metal production, operational challenges must be overcome. Strong and reactive precursor pellets are necessary to effectively and selectively produce $Mg_{(g)}$ from any feedstock. In this study, the effects of ore (magnesia and dolime), carbon (petroleum coke, charcoal, algal char, and carbon black), and binder (organic and inorganic) on pellet strength and reactivity, product yield and purity, and reduction selectivity were analyzed. Theoretically and experimentally, the CTR of dolime (MgO·CaO) favored MgO reduction over CaO reduction; however, with enough carbon and heat, both oxides could be reduced. CaO carbothermal reduction produced CaC_2 and $Ca_{(g)}$. The selectivity to CaC_2 remained constant (7 ± 4 pct) for all C/MgO·CaO ratios analyzed, while the selectivity to $Ca_{(g)}$ increased (5 pct → 40 pct) when C/MgO·CaO was increased from 0.5 to 2.0. As the overall metal yield decreased (77.6 pct → 59.7 pct) with increasing CaO reduction (38.2 pct → 78.1 pct), $Ca_{(g)}$ reverted faster than $Mg_{(g)}$. Heavy metal impurities primarily remained in the residue (< 30 pct volatilized) and, when volatilized, condensed at high temperatures (700 °C to 1450 °C), relative to light metal impurities (350 °C to 1000 °C, > 78 pct volatilized). Organic binders added reducing power to the pellets but produced frail pellets (radial crush strength = 9.1 ± 0.7 N) after pyrolysis, relative to pellets with inorganic binders (15.1 ± 3.2 N). Kinetic parameters were determined for extruded pellets to predict the reaction rate as a continuous function of pressure and temperature.

https://doi.org/10.1007/s11663-018-1309-5

I. INTRODUCTION

MAGNESIUM metal production by carbothermal reduction can be an economic and clean alternative to current production methods (electrolytic, silicothermic) because of the low theoretical energy requirement (7.5 kWh/kg).[1] The high-temperature (> 1000 °C) reaction produces magnesium as a gas.

$$C + MgO \leftrightarrow CO + Mg_{(g)} \quad [1]$$

During the years surrounding WWII, the Permanente plant produced magnesium using this chemistry,[2] but low yields and operational challenges prevent that process from being profitable today. For the effective generation of $Mg_{(g)}$, pellets dropped into the reactor should be physically strong to resist thermal and physical shocks, should quickly reduce MgO, and should volatilize minimal impurities. The effects of ore (dolime, magnesia), carbon (petroleum coke, algal char, charcoal, carbon black), and binder (organic, inorganic) on pellet strength, reduction rate, product selectivity, and magnesium yield were investigated.

Natural mineral sources of magnesium ore include dolomite, magnesite, brucite, carnallite, and olivine (among others).[3] Magnesium hydroxide can be precipitated out of salt water brines when mixed with lime or other precipitating agents.[4] Dolomite (MgO·CaO·$(CO_2)_2$) is the primary ore for magnesium production by silicothermic reduction, forming Ca_2SiO_4 as a byproduct. Researchers have studied magnesium production by the CTR of calcined dolomite under the assumption that CaO does not react with C[5–7]; however, Winand *et al.*[8] observed 10 pct CaO reduction for 60 pct MgO reduction at 1427 °C. The effect of pellet stoichiometry (C/MgO·CaO) on product yield and selectivity for the CTR of calcined dolomite at 1550 °C and 10 kPa is presented in this study.

BORIS A. CHUBUKOV, SCOTT C. ROWE, KEVIN Y. SUN, and ALAN W. WEIMER are with the Department of Chemical and Biological Engineering, University of Colorado Boulder, Boulder, CO 80309-0596. Contact e-mail: alan.weimer@colorado.edu AARON W. PALUMBO and MARK A. WALLACE are with the Department of Chemical and Biological Engineering, University of Colorado Boulder and also with Big Blue Technologies LLC, Westminster, CO 80020.

Manuscript submitted November 22, 2017.
Article published online June 14, 2018.

Suitable sources of carbon for magnesium production by CTR include petroleum coke, coal, and charcoal (among others).[1] Previous studies have shown that the rate of CTR depends on the composition of impurities within the carbon source[9–13] but have not investigated the fate of impurities. Here, four carbon sources were used to determine the relative reactivity of each material and the resultant product impurity profile.

Strong pellets are necessary to prevent attrition during transportation and to maintain bed structure during reduction. For iron ore reduction in a blast furnace, high-temperature sintering of iron ore produces a strong pellet. The same concept could be employed for MgO carbothermal reduction; however, the reduction rate would be incredibly slow, and the high concentration of oxidative CO_2 in the effluent of a blast furnace would result in almost complete reversion of product $Mg_{(g)}$.[14] Instead, reduction under vacuum improves Mg yield as CO is the primary byproduct. Carbothermal reduction of magnesia at pressures ≤ 10 kPa results in high $Mg_{(s)}$ yield (> 85 pct) when product $Mg_{(g)}$ is condensed heterogeneously at high temperatures (> 450 °C).[15–17] The current study was operated in this regime.

Efficient carbon and magnesium oxide particle contact is crucial to propagate the reaction under vacuum. Here, carbon and magnesium oxide powders were pelletized together to improve particle contact, contrary to iron ore processing. In addition, ball-milling carbon and magnesium oxide powders prior to pelletizing can further increase particle contact.[18,19] These methods have been successfully employed by researchers to promote the carbothermal reduction reaction.[2,15,16,19,20] Without whole pellet sintering, a binder may be necessary to maintain pellet strength. The effect of pyrolysis temperature on pellet strength and reactivity was studied using organic and inorganic binders. To characterize effective pellets, a kinetic model, based on a macroscopic species balance,[15] was fitted to experimental data to predict the reaction rate as a continuous function of temperature and pressure.

II. METHODS

A. *Materials*

Table I summarizes the raw materials used in this study. Dolomite core drillings from Nevada Clean Magnesium, Inc. were of 2 to 10 cm in size. These samples were hand-crushed to < 0.5 cm and then wet milled in anhydrous ethanol for 60 minutes. The resulting powder was vacuum calcined (46.7 pct mass loss) at 750 °C and 0.1 kPa. Petroleum coke from Marathon Petroleum was in the form of 0.5 to 10 cm agglomerates, and charcoal from Kingsford was in the form of 5.7 cm briquettes; both samples were hand-crushed to < 0.5 cm and dry milled for 60 minutes. Spray-dried *Chlorella* (microalgae) from Arizona Public Services was pyrolyzed at 650 °C in N_2, and the char was pulverized by mortar and pestle. All other samples were used as received.

B. *Material and Pellet Processing*

Dry and wet milling was performed using an HD-01 attritor from Union Process. Stainless steel balls (440c, 3.175 mm diameter) loaded into a 1.0 L canister, media:powder = 10:1 (mass basis), pulverized the sample at 708 RPM.

Pelletization was performed using three methods: molding, briquetting, and extruding. For molding, powders were dry mixed in a rotary mixer and then formed into a paste by the addition of water (~ 1 mL/g). This paste was pressed into 6.35-mm spherical molds in a silicone support. The filled molds were dried at 105 °C for 12 hours after which hardened pellets were removed. Briquettes were dry formed using a hydraulic press and a 6.00 mm or 25.4 mm die by applying 20 kN of force. Extrusions were formed using a D150G pellet mill in which two cylinders forced powder material through a rotating steel die plate with 3.0-mm holes. A blade at the exit of the rotating die cut extrusions to 12 mm. To lubricate the flow of material, 200 mL of oil was added per 1 kg of C/MgO powder. All pellets were pyrolyzed at 650 °C in N_2 and then stored in a vacuum desiccator prior to use. To assess the relative reactivities of pellets made by each method, pellets were made with petroleum coke and magnesia following C/MgO = 1.0 (molar).

C. *Experimental Procedure*

Pellet reactivity was determined by measuring product gas (CO/CO_2) evolution upon dropping 1.0 g of C/MgO pellets into a hot SiC (Hexoloy SA) crucible within a graphite furnace at isothermal and isobaric conditions. Although the reduction of MgO by SiC can proceed under these conditions, no pitting was observed in the relatively inert crucible. Product magnesium condensed on a removable graphite liner within a radiantly cooled 2.54-cm-OD alumina tube. The experimental procedure and apparatus are described in detail by Chubukov *et al.*[15] Time-dependent conversion ($\alpha(t)$) of MgO to $Mg_{(g)}$ was determined by the molar flow rates of CO ($\dot{N}_{CO}$) and CO_2 ($\dot{N}_{CO_2}$) after correcting for reversion, Eq. [2], and dispersion.[15,21] Yield (Y) was defined as the fraction of $Mg_{(s)}$ condensed relative to $Mg_{(g)}$ formed, Eq. [3], based on the moles of CO and CO_2 released and the moles of MgO reacted $\left(N_{MgO,Initial} - N_{MgO,Final}\right)$. Carbon monoxide composed the majority (> 98 pct) of the product gas stream.

$$\alpha(t) = \frac{\int_0^t \left(\dot{N}_{CO} + 2\dot{N}_{CO_2}\right) dt}{Y \cdot N_{MgO,Initial}} \quad [2]$$

$$Y = \frac{\int_0^{t_{final}} \left(\dot{N}_{CO} + 2\dot{N}_{CO_2}\right) dt}{N_{MgO,Initial} - N_{MgO,Final}} \quad [3]$$

For the case of dolime (MgO·CaO), the yields of $Mg_{(s)}$ and $Ca_{(s)}$ from $Mg_{(g)}$ and $Ca_{(g)}$ could not be determined independently based on the CO/CO_2 signal, and condensate composition inaccurately reflected the yield

Table I. Raw Materials Used in This Study

Category	Supplier	Material	SSA (m^2/g)
Ore	Premier Magnesia LLC	magnesia	147
	Nevada Clean Magnesium (NCM)	dolomite	99.4**
	Charles B Chrystal Co. (CBC)	dolime	0.220
Carbon	Marathon Petroleum	petroleum coke	7.78**
	Soltex	carbon black	85.3
	Arizona Public Services	spray-dried microalgae	0.0409*
	Kingsford	charcoal	196**
Binder	Best Bentonite	bentonite	23.4
	Archer Daniels Midland (ADM)	wheat starch	0.362
	Alfa Aesar	lime	15.6
	Brer Rabbit	molasses	liquid

*Material was pyrolyzed. **Material was pyrolyzed and milled for 60 min.

because of product oxidation in air prior to analysis. Instead, an overall metal yield was calculated based on the total oxygen balance.

The selectivity (S_i) of dolime carbothermal reduction to $Mg_{(g)}$, $Ca_{(g)}$, or CaC_2 was defined by Eq. [4], where N_i refers to the moles produced of each species based on the composition of the residue.

$$S_i = \frac{N_i}{\left(N_{\mathrm{MgO,Initial}} + N_{\mathrm{CaO,Initial}}\right) - \left(N_{\mathrm{MgO,Final}} + N_{\mathrm{CaO,Final}}\right)} \quad [4]$$

The selectivity, overall metal yield, reduction extent, and reaction rate for the CTR of calcined dolomite (NCM) were determined experimentally for C/MgO·CaO molar ratios of 0.5, 1.0, 1.5, and 2.0 in 6.0 mm briquettes using petroleum coke as the carbon source. Thermodynamic predictions for the products of these reactions were determined by Gibbs free energy minimization using *FactSage 7.1*.[22]

To determine the impurity profile of product Mg using various carbon sources, a relatively large mass (150 g) of pellets was reacted to improve the recovery of trace metals. Pellets were made with magnesia following C/MgO = 1.0 (molar) and pressed into 25.4 mm diameter briquettes using 10 pct starch as binder. Pellets were pyrolyzed in N_2 at 650 °C prior to reaction. Once loaded, the furnace temperature was raised to 650 °C at 5 °C/minute under a vacuum of 10 kPa and held there for 4 hours to remove any adsorbents. Argon sweep gas (1 slm) maintained the gas path. The furnace temperature was then raised to 1550 °C at 10 °C/minute and held for 3.5 hours. Product magnesium condensed on a removable graphite foil lining the inside of the SiC crucible. A mass spectrometer (SRS QMS 200) and nondispersive infrared detector (Nova 7905 AH) were used to measure the product gas composition. The rates of CO emission from these experiments were equal for all carbon sources, indicating that the reaction was heat transfer limited. Therefore, the relative reaction rates using various carbon sources were determined by dropping 1.0 g of molded pellets into the crucible following the protocol described earlier. The reaction using this relatively small mass was not subject to significant heat transfer limitations, and kinetic comparisons could be made.

To study the effect of organic and inorganic binders, starch and molasses were used as organic binders, and bentonite and lime were used as inorganic binders. Organic (10 pct starch) and organic–inorganic (5 pct starch-5 pct bentonite, 8 pct molasses-2 pct lime) binders were selected based on previous studies[23–25] that demonstrated their success. Pellets were made by molding using carbon black and magnesia or dolime (CBC) following C/MgO = 1.2 (molar).

D. *Material Characterization*

Elemental composition of trace impurities was measured using ICP-MS and ICP-OES. Carbon and oxygen elemental compositions were determined using LECO instruments C200 and TC600, respectively. For dolime pellets, MgO/CaO/CaC_2 content was estimated by XRD analysis (Bruker D2 Phaser) using the Rietveld method.[26] Radial crush strength was determined according to ASTM D4179-11.[27] Powder's specific surface area was measured by BET (Micromeritics Gemini V). Imaging was performed by field emission scanning electron microscopy (FESEM) using a JEOL 7401 F microscope. Thermogravimetric analysis (TGA) was performed using a Netzsch STA 449 F1 Jupiter.

III. RESULTS AND DISCUSSION

A. *Theoretical Predictions for the Carbothermal Reduction of Calcined Dolomite*

Figure 1 shows thermodynamic predictions for the carbothermal reduction of calcined dolomite at a product gas pressure of 10 kPa. Based on these predictions, complete conversion of MgO to $Mg_{(g)}$ occurs at 1535 °C, while CaO reduction at this temperature is < 1 pct. Carbon reacts completely at 1627 °C forming carbon monoxide and calcium carbide. Further increasing temperature favors calcium reduction to $Ca_{(g)}$. At 1776 °C, calcium and magnesium are completely reduced, and the products are CO, $Mg_{(g)}$, and $Ca_{(g)}$.

These closed system predictions indicated that, in addition to Reaction [1], the following independent reactions will likely take place during the CTR of calcined dolomite:

$$CaO + C \leftrightarrow Ca_{(g)} + CO \quad [5]$$

$$CaO + 3C \leftrightarrow CaC_2 + CO \quad [6]$$

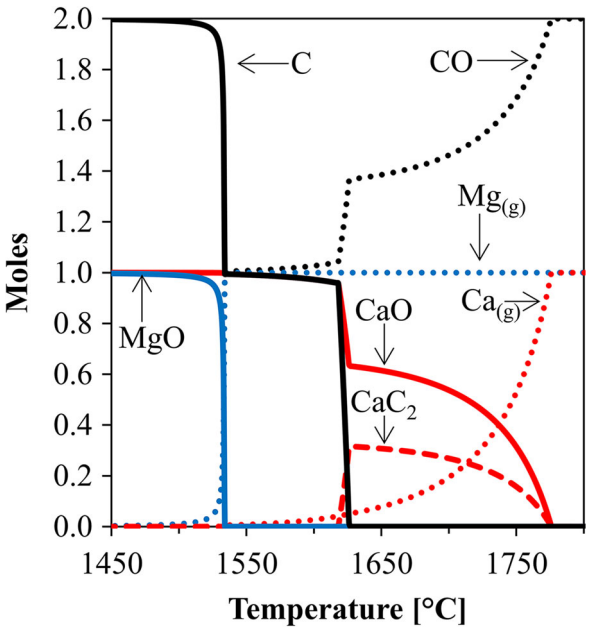

Fig. 1—Thermodynamic prediction for products of 2C + MgO·CaO at a product gas pressure of 10 kPa.

B. *Experimental Results for the Carbothermal Reduction of Calcined Dolomite*

Figure 2 illustrates the extent of MgO and CaO CTR, the selectivity of CTR, the rate of CO emission, and the overall metal yield of $Mg_{(s)}$ and $Ca_{(s)}$ for reaction at 1550 °C and 10 kPa. For C/MgO·CaO ratios of 0.5 and 1.0, CTR favored MgO reduction ($S_{Mg} = 0.87 \pm 0.10$). Carbon reduced MgO completely at ratios of 1.5 and 2.0, allowing for further CaO reduction. For C/MgO·CaO = 2.0, carbon reduced 78.1 ± 2.5 pct of CaO, even though thermodynamic predictions indicated < 1 pct conversion at this temperature. Vacuum and argon flow maintained the product gas partial pressures below that of reaction equilibrium, allowing for high conversion. Further, effective particle contact by compacting high surface area powders, as was the case for these experiments, has previously been shown to lower the onset temperature for CTR.[13,18,28]

The CTR of calcined dolomite produced $Mg_{(g)}$, $Ca_{(g)}$, and CaC_2. Calcium carbide selectivity remained fairly constant across all ratios ($S_{CaC_2} = 0.07 \pm 0.04$), while the selectivity for $Ca_{(g)}$ increased with C/MgO·CaO. CaC_2 is produced industrially by CaO CTR in an open electric arc furnace at high temperatures (> 2000 °C).[29] The use of vacuum in this system favored reduction at lower temperatures and production of $Ca_{(g)}$.

For all ratios, the majority of CO emission (> 85 pct) occurred within the first 20 minutes of reduction, and the reduction was complete after 60 minutes. The overall metal yield remained high (≥ 75.0%) with increasing C/MgO·CaO, but dropped (59.7 ± 0.3 pct) for C/MgO·CaO = 2.0. Because of the decrease in yield,

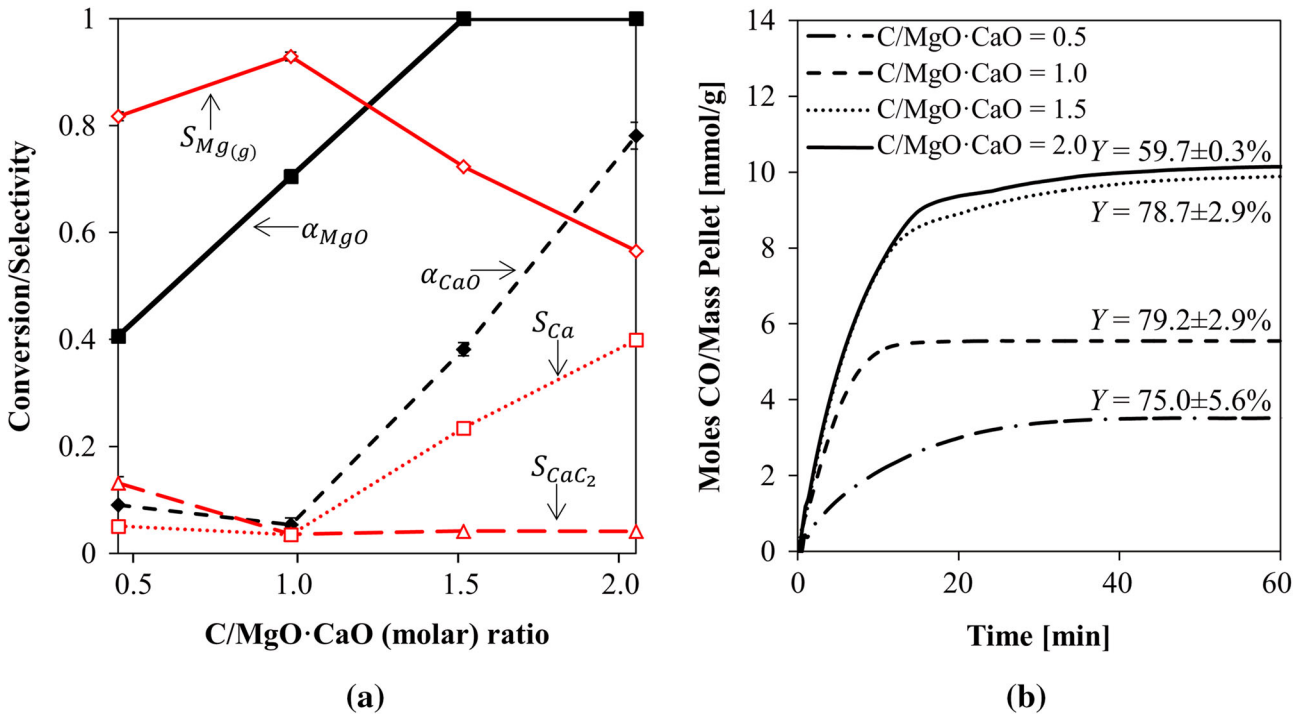

Fig. 2—(*a*) Conversion, α, and selectivity, *S*; and (*b*) normalized CO emission rate and yield for the CTR of MgO·CaO at 1550 °C and 10 kPa.

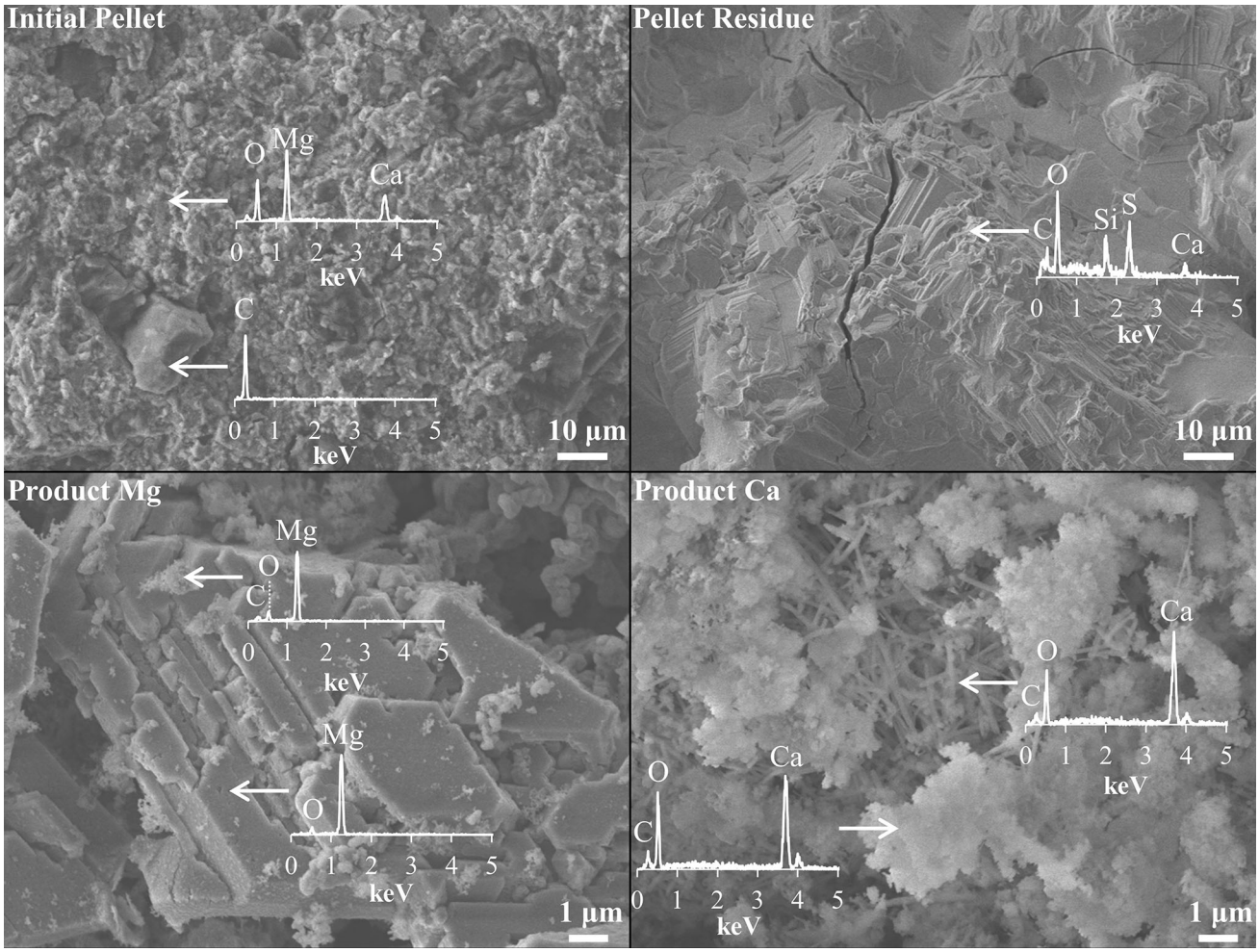

Fig. 3—SEM images of initial pellet, pellet residue, product Mg, and product Ca from the CTR of C/MgO·CaO = 2 (molar) at 1550 °C and 10 kPa. EDS spectra are overlapped, and arrows identify the analyzed point.

we concluded that $Ca_{(g)}$ reverted more readily than $Mg_{(g)}$. When the pellets were carbon limited (C/MgO·CaO < 2), carbon was primarily consumed by MgO reduction, and the yield remained high as $Mg_{(g)}$ was the favored product. For stoichiometric pellets (C/MgO·CaO = 2.0), after complete reduction of MgO, the reduction of CaO proceeded, and the yield dropped because of the relatively large amount of $Ca_{(g)}$ produced.

Figure 3 shows SEM images of reactant, residue, and products from the CTR of C/MgO·CaO = 2.0. The initial pellet was a dense compact of C and MgO·CaO; 10 to 20 μm carbon particles were embedded in the calcined dolomite. After the reaction, the residue was sintered and showed areas of crystallinity. The residue was composed of unreacted CaO and product CaC_2, identified by XRD, and Si and S impurities, identified by EDS.

Product gases condensed in two distinct bands. The location of the first band corresponded to a condensation temperature of 1400 °C to 1150 °C and appeared white to the eye. The band was composed of calcium metal, identified by XRD, and calcium oxide and carbon from reversion, identified by EDS. The calcium metal appeared as needle-shaped crystals, while the reversion product (C/CaO) appeared as an amorphous cluster. This condensation zone is labeled 'Product Ca' in Figure 3. The location of the second band corresponded to a condensation temperature of 700 °C to 500 °C and appeared gray to the eye. This band showed Mg metal in hexagonal grains (10 to 100 μm). Clusters of reversion product (C/MgO) and surface oxidation of $Mg_{(s)}$ were visible. This condensation zone is labeled as 'Product Mg'.

C. *Carbon*

The composition of the effluent as measured by mass spectrometry showed that the only gases evolved above 650 °C were H_2, CO, and CO_2. Table II and Figure 4(a) show the impurity profile and reactivity of each carbon source, respectively. Petroleum coke, charcoal, and carbon black reduced MgO at a similar rate (> 80 pct conversion in 30 minutes) while reduction by algal char was relatively slow (57 pct conversion in 30 minutes) because of its low specific surface area. SEM images in

Table II. Impurity Profiles of Carbon Sources

Reductant	Fixed C (Pct)	Impurities (ppm)								
		Fe	Ni	Ca	Mn	Zn	Si	K	Na	Al
Carbon Black	> 99 pct	529	32	3571	80	18	1298	< 5	161	141
Petroleum Coke	90.8 ± 0.5	611	20	3717	92	13	947	< 5	102	112
Charcoal	65.6 ± 1.0	848	17	30001	150	20	6730	589	1269	1162
Algal Char	67.1 ± 2.6	571	17	3740	85	14	1417	4356	128	152

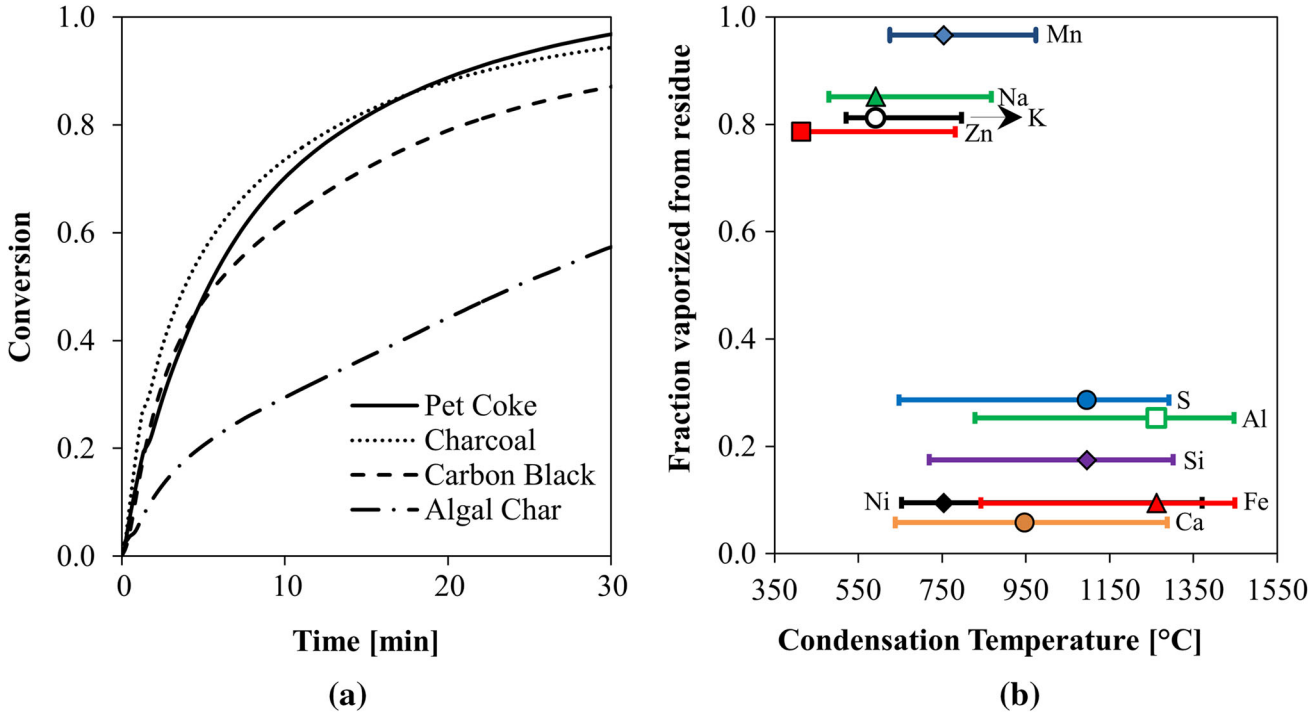

Fig. 4—(*a*) Reactivity of MgO CTR at 1550 °C and 1 kPa using four carbon sources for C/MgO = 1.0 (molar). (*b*) Deposition profile of impurities from MgO CTR at 1550 °C and 10 kPa. Points represent the highest deposition concentration, and bars encompass 75 pct of total deposits averaged over the four carbon sources.

Figure 5 show that algal char particles were 10 to 200 μm, petroleum coke and charcoal powders were < 10 μm, and carbon black powders were < 100 nm. As charcoal and algal char compositions were similar, milling the algal char would likely improve its reactivity.

The reaction rate depends on the specific surface areas of carbon and magnesia,[13] the C/MgO particle contact,[28,30] the composition of metal impurities which can catalyze the reaction,[10,13] and other parameters.[15] Charcoal had the highest specific surface area and impurity composition but did not demonstrate exceptional reactivity over petroleum coke or carbon black. Similarly, reduction experiments by Rongti *et al.*[30] showed little difference in reaction rates when using charcoal or graphite powers as the reducing agent. General reactivity trends have been observed in controlled experiments, but it remains difficult to predict the reactivity of a pellet solely based on the properties of the raw materials.

The deposition profile of impurities was similar for each carbon source. Figure 4(b) illustrates the averaged deposition profiles from the four carbon sources. High boiling point metals (Fe, Ni, Si, Al) and stable oxides (CaO) primarily remain in the pellet residue (< 30 pct volatilized) and condensed at high temperatures (700 °C to 1450 °C) when volatilized. Lighter metals (Zn, K, Na, Mn) volatilized easily (> 78 pct volatilized) and condensed at a lower temperature (350 °C to 1000 °C). Light metal impurities condensing within the same region as Mg (< 650 °C) would be difficult to separate during the initial condensation, and thus further purification may be necessary. Vacuum distillation, although

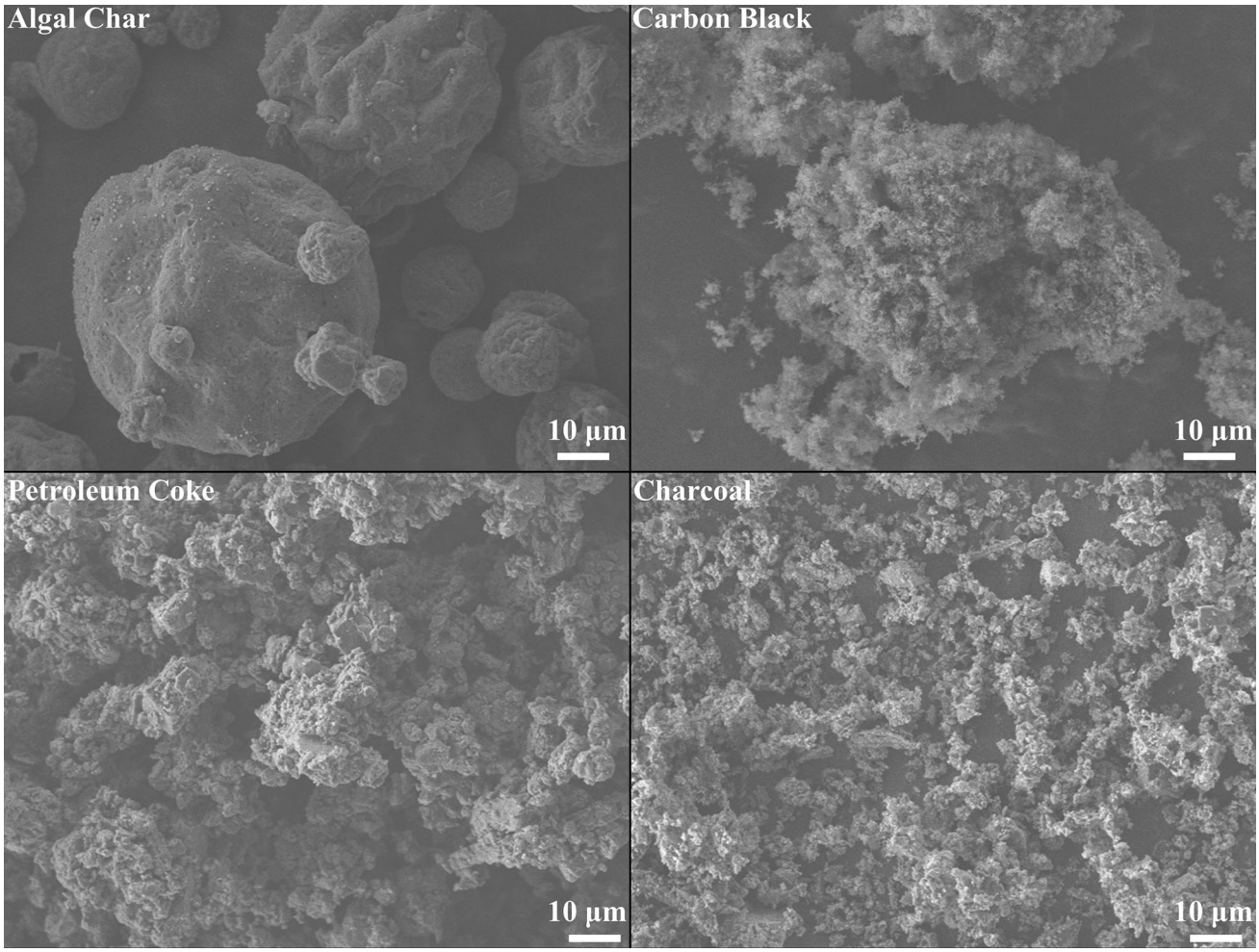

Fig. 5—SEM images of carbon sources.

energy intensive, has proven to produce a clean Mg product.[17]

D. *Binder*

Partial or complete pyrolysis of binder can be beneficial before adding pellets to the reactor because pyrolysis gases (CO, CO_2, H_2O) will oxidize $Mg_{(g)}$. Figure 6(a) illustrates pellet strength and mass loss for pyrolysis temperatures from 250 °C to 650 °C. For pellets made with MgO, the extent of pyrolysis approached the weight loading of the organic binder with increasing temperature indicating significant binder decomposition. For pellets made with dolime, the mass loss of pellets exceeded the weight loading of the organic binder at pyrolysis temperatures ≥ 350 °C. Hydration of CaO in dolime during pelletizing resulted in subsequent dehydration during pyrolysis. This hydration can be avoided by dry briquetting or oil-based extruding. Many small-scale studies[10,16,20,28,30,31] successfully dry briquetted C and MgO powders to form compacts.

Figure 6(b) illustrates pellet strength after pyrolysis at temperatures up to 650 °C. Pellets made with molasses-lime were frail (< 15 N) under all tested conditions. Magnesia pellets made with starch and starch-bentonite as the binder were strong initially (38 to 67 N) but weakened after pyrolysis at 250 °C because of organic binder decomposition. Dolime pellets maintained their strength until 450 °C because of the cementitious properties of hydrated CaO. After pyrolysis at 650 °C, dolime and magnesia pellets exhibited similar strengths: starch-bentonite = 15.1 ± 3.2 N, starch = 9.1 ± 0.7 N, molasses-lime = 1.6 ± 0.2 N. The improved strength of starch-bentonite over starch pellets indicated that, as the organic component decomposed to char, the inorganic component maintained pellet strength. All pellets resisted the physical and thermal shocks of being dropped into the reactor, but the residue easily crumbled when handled.

Pellet reactivity was assessed at 1550 °C and 1 kPa, Figure 7. Although the initial (0 to 5 minutes) rate of CO emission was similar for all pellets (1.60 ± 0.19 $mmol/g_{Pellet}/minute$), the overall CO emitted followed the weight loading of the organic binder. Char from pyrolysis of organic binder increased the C/MgO ratio within the pellet which added to the reduction potential. Pellets made with 10 pct starch showed the greatest CO emission. The reduction of dolomitic pellets was carbon limited, indicating some reduction of CaO, and the reaction was complete after 12 minutes.

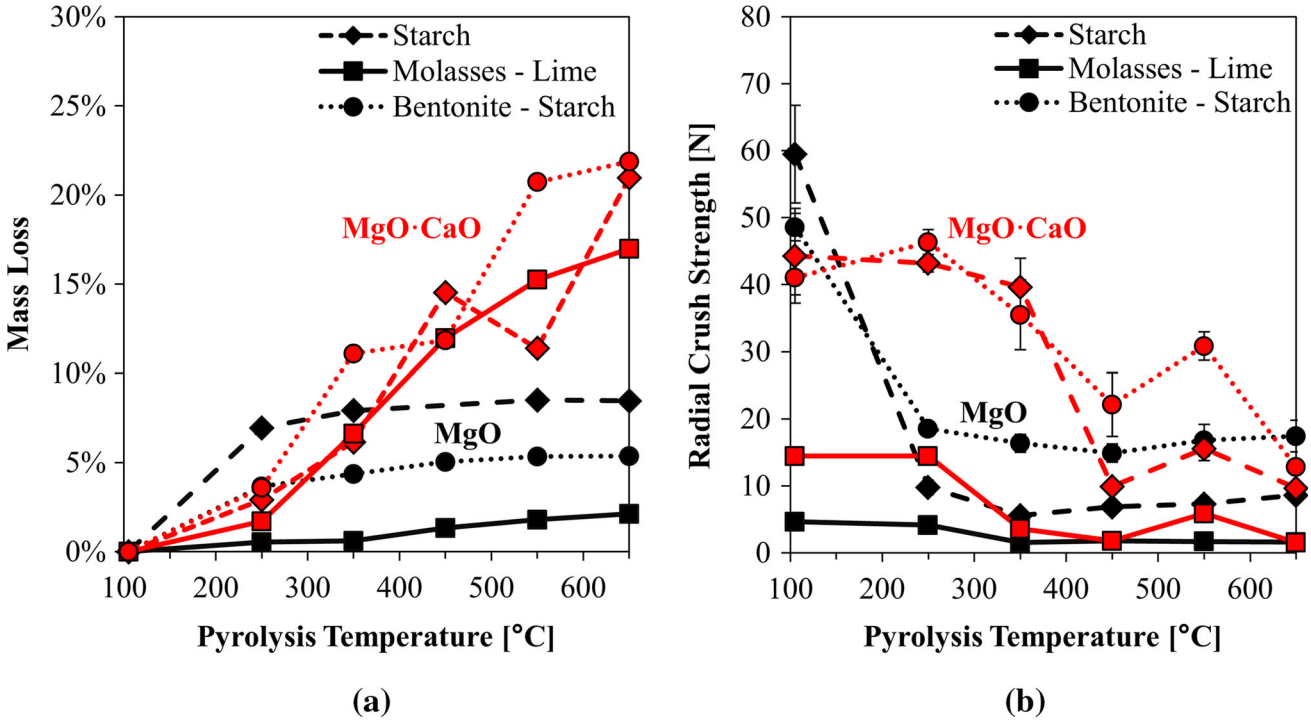

Fig. 6—(*a*) Mass loss of magnesia (MgO) and dolime (MgO·CaO) pellets made with organic and/or inorganic binders, and (*b*) radial crush strength of pellets after pyrolysis.

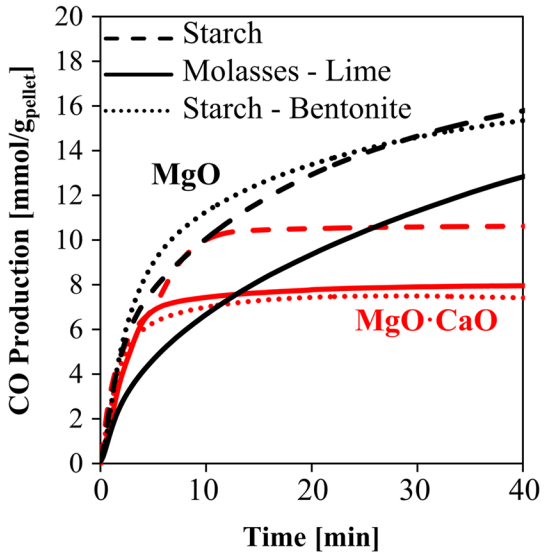

Fig. 7—Product gas (CO) evolution for CTR of magnesia and dolime at 1550 °C and 1 kPa.

The molding method produced fairly weak pellets as no compaction force was applied, but the trends observed here can be applied to other pelletization methods to produce effective pellets for CTR.

E. *Pelletization*

Figure 8(a) shows the reduction rates at 1550 °C and 1 kPa for pellets made by each pelletization method. The reactivities of extruded and molded pellets were similar, while the initial reactivity of briquettes was relatively slow; however, a similar extent of conversion was reached by all pellets after 30 minutes of reaction (96.6 ± 0.5 pct). The addition of a liquid while molding or extruding pellets produced a porous pellet, relative to briquetting, which allowed product gases to escape. The initial reactivity of the briquettes was likely limited by mass transfer of product gases out of the pellet. The organic component of petroleum coke functioned as an excellent binder, and briquettes and extrusions were strong even after pyrolysis.

F. *Kinetic Modeling*

For further MgO CTR process development, pellets were made by extrusion using petroleum coke and magnesia. These pellets were strong, could be produced quickly and in large quantities, and required no additional binder. Kinetics of these pellets were measured as a function of temperature and pressure using a 2^2 factor design with a center-point. Within the experimental space, the reactivity increased with vacuum and temperature, and the rate could be adequately described by a reversible rate law for Reaction [1], Eq. [7] and [8].

$$r_1 = A_0 e^{-\frac{E_a}{RT}} \cdot A_{ss} \cdot \left(1 - \frac{p_{CO} p_{Mg}}{K_{eq}}\right) \qquad [7]$$

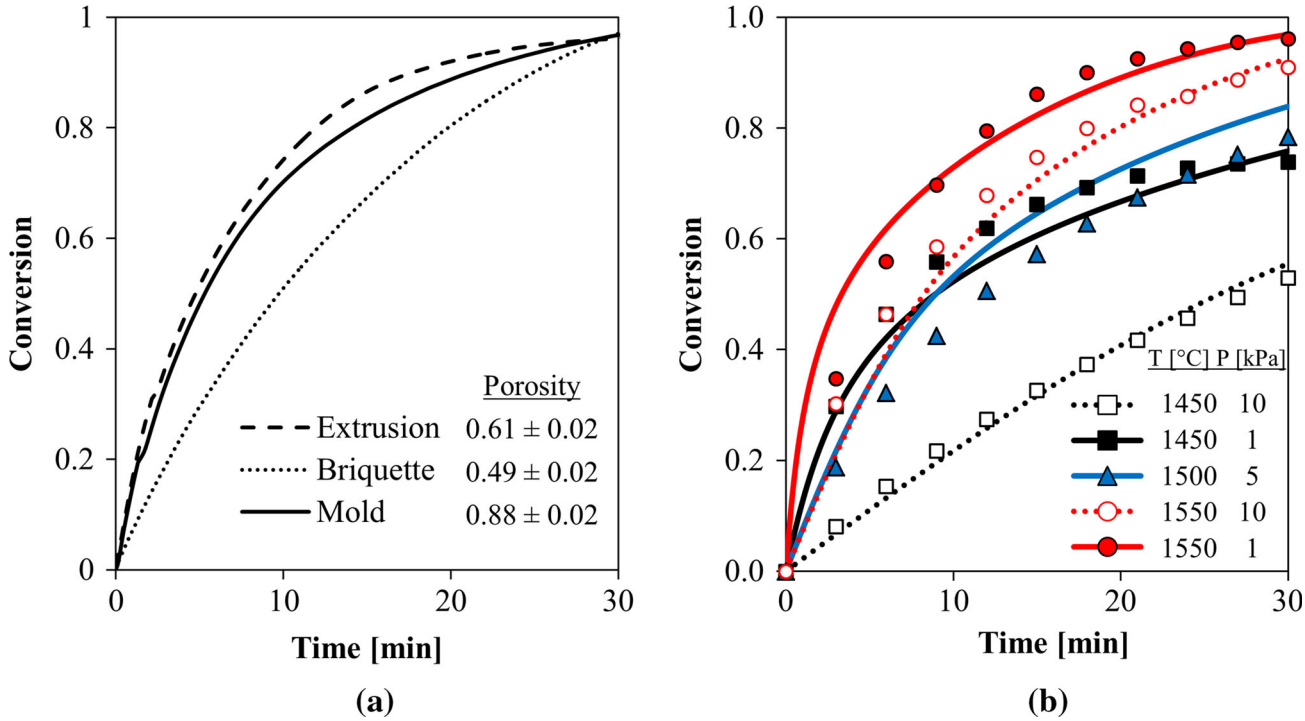

Fig. 8—(*a*) MgO CTR at 1550 °C and 1 kPa for equimolar pellets made using petroleum coke and magnesia, and (*b*) kinetic measurements (points) for MgO CTR for extruded pellets. Model fits are shown as lines.

$$A_{ss} = A_{MgO}\left(x_p(1-\alpha)^{2/3} + (1-x_p)(1-\alpha)^{x_k}\right), \quad [8]$$

The rate was derived assuming that the solid–solid reaction between C and MgO is rate limiting, and that the gas–solid reactions of $C + CO_2 \rightarrow 2CO$ and $MgO + CO \rightarrow Mg + CO_2$ are negligible. The reaction rate (r_1) is given in Eq. [7] as a function of temperature (T), product gas partial pressures (p_{CO} and p_{Mg}), and conversion (α). The dependence of rate on temperature is given by an Arrhenius rate expression and the equilibrium constant (Keq). The effect of conversion is captured by the decreased in area of solid–solid particle contact (A_{ss}) given by Eq. [8].

Equation [8] represents the reduction of C/MgO particle contact with conversion scaled by the specific surface area of the magnesia (A_{MgO}). The first term follows a shrinking core reduction, while the second term gives a faster decay in surface area with conversion ($x_k > 2/3$). The weight of each term is given by x_p. For further discussion on the model development and methods to estimate product gas partial pressures, the reader is referred to the author's previous study.[15]

The parameters A_0, E_a, x_p, and x_k were fitted to experimental results by nonlinear least squares regression, and the resulting parameter values were $A_0 = 27.2$ [mol/m^2/s], $E_a = 250$ [kJ/mol], $x_p = 8.00 \times 10^{-2}$, and $x_k = 4.33$. Figure 8(b) shows the model fit. The macroscopic species balance model was initially developed for molded pellets of carbon black and magnesia,[15] and the model adequately predicted the reaction rate for the extruded pellets with revised rate parameters.

IV. CONCLUSION

Ore (magnesia, dolime), carbon (petroleum coke, algal char, charcoal, carbon black), and binder (organic, inorganic) materials were studied for Mg production by carbothermal reduction (CTR). The CTR of dolime favored MgO reduction over CaO reduction theoretically and experimentally. However, when enough carbon was present in the pellets, both oxides were reduced at 1550 °C and 10 kPa producing $Mg_{(g)}$, $Ca_{(g)}$, and CaC_2. When both MgO and CaO were reduced, the overall metal yield was lower than when primarily MgO was reduced. This indicated that $Ca_{(g)}$ reverted more readily than $Mg_{(g)}$.

The pyrolytic decomposition of organic binder increased the reducing power of C/MgO pellets but resulted in frail pellets relative to those made with inorganic binders. However, the carbon source had little effect on the reactivity of pellets, except in the case of algal char as the specific surface area was very low. Likewise, the pelletization method (molding, briquetting, extruding) used to form C/MgO pellets only

affected the initial reactivity of pellets, and all pellets reached > 95 pct conversion after 30 minutes of reaction at 1550 °C and 1 kPa.

For all carbon sources tested, the impurity profile in the residue and product Mg showed similar trends. Heavy metal impurities primarily remained in the pellet residue while lighter metals significantly contaminated the product Mg.

For a given pellet recipe and pelletization method, rate parameters can be fitted to predict the reaction rate with temperature and pressure. Here, we fitted rate parameters to extruded pellets of petroleum coke and magnesia as a continuous function of temperature and pressure.

ACKNOWLEDGMENTS

The authors acknowledge the financial support from the National Science Foundation: Award 1622824, and from the Advanced Research Projects Agency-Energy (ARPA-E) of the US Department of Energy (DOE): Award AR0000404. Dragan Mejic provided machining, welding, and design services for all custom vacuum hardware. Dave Sorenson at Dover Resources provided carbon consulting services.

CONFLICT OF INTEREST

Boris Chubukov, Scott Rowe, and Aaron Palumbo are co-founders of Big Blue Technologies and are working to commercialize magnesium production by carbothermal reduction.

REFERENCES

1. S. Trang, G. Brooks, P. Witt, M.N.H. Khan, and M. Nagle: *JOM*, 2006, vol. 58, pp. 51–55.
2. F.J. Hansgirg: *Iron Age*, 1943, vol. 18, pp. 56–63.
3. D.A. Kramer: *USGS Minerals Yearbook*, vol. 47, 2005.
4. O. Söhnel and J. Mareček: *Cryst. Res. Technol.*, 1978, vol. 13, pp. 253–62.
5. C.-B. Yang, Y. Tian, T. Qu, B. Yang, B.-Q. Xu, Y.-N. Dai, and J. Magnes: *Alloys*, 2013, vol. 1, pp. 323–29.
6. S. Wang, G. Bin, Y. Wang, and J. Diao: *Magnes. Technol.*, 2014, vol. 2014, pp. 43–47.
7. W.-D. Xie, J. Chen, H. Wang, X. Zhang, X.-D. Peng, and Y. Yang: *Rare Met.* 2014, pp. 1–6.
8. R. Winand, M. Van Gysel, A. Fontana, L. Segers, and J.C. Carlier: 1990.
9. A. Berman and M. Epstein: *J. Phys. IV*, 1999, vol. 9, pp. 319–24.
10. L. Rongti, P. Wei, M. Sano, and J. Li: *Thermochim. Acta*, 2003, vol. 398, pp. 265–67.
11. M.E. Galvez, A. Frei, G. Albisetti, G. Lunardi, and A. Steinfeld: *Int. J. Hydrogen Energy*, 2008, vol. 33, pp. 2880–90.
12. Y. Jiang, H.W. Ma, and Y.Q. Liu: *Advanced Materials Research*, Trans Tech Publ, Zürich, 2013, pp. 2552–55.
13. B.A. Chubukov, A.W. Palumbo, S.C. Rowe, M.A. Wallace, and A.W. Weimer: *Ind. Eng. Chem. Res.*, 2017, vol. 56 (46), pp. 13602–09.
14. I. Hischier, B.A. Chubukov, M.A. Wallace, R.P. Fisher, A.W. Palumbo, S.C. Rowe, A.J. Groehn, and A.W. Weimer: *Sol. Energy*, 2016, vol. 139, pp. 389–97.
15. B.A. Chubukov, A.W. Palumbo, S.C. Rowe, I. Hischier, A.J. Groehn, and A.W. Weimer: *Thermochim. Acta*, 2016, vol. 636, pp. 23–32.
16. L.H. Prentice, M.W. Nagle, T.R.D. Barton, S. Tassios, B.T. Kuan, P.J. Witt, and K.K. Constanti-Carey: *Magnesium Technology 2012*, Wiley, New York, 2012, pp. 29–35.
17. Q. Tao, B. Yang, Y. Tian, and Y. Dai: *Magnesium Technology 2015*, Wiley, New York, 2015, pp. 55–59.
18. M. Nusheh, H. Yoozbashizadeh, M. Askari, N. Kuwata, J. Kawamura, J. Kano, F. Saito, H. Kobatake, and H. Fukuyama: *ISIJ Int.*, 2010, vol. 50, pp. 668–72.
19. B.A. Chubukov, A.W. Palumbo, S.C. Rowe, M.A. Wallace, and A.W. Weimer: *Ind. Eng. Chem. Res.*, 2017, vol. 56, pp. 13602–09.
20. O.P. Solonenko, A.V. Smirnov, A.E. Chesnokov, V.A. Poluboyarov, and A.A. Zhdanok: *Thermophys. Aeromech.*, 2016, vol. 23, pp. 451–59.
21. J.R. Scheffe, A.H. McDaniel, M.D. Allendorf, and A.W. Weimer: *Energy Environ. Sci.*, 2013, vol. 6, pp. 963–73.
22. C.W. Bale, E. Bélisle, P. Chartrand, S.A. Decterov, G. Eriksson, A.E. Gheribi, K. Hack, I.-H. Jung, Y.-B. Kang, and J. Melançon: *Calphad*, 2016, vol. 54, pp. 35–53.
23. T.D. Taulbee, D.P. Patil, R.Q. Honaker, and B.K. Parekh: *Int. J. Coal Prep. Util.*, 2009, vol. 29, pp. 1–22.
24. A.P. Zambrano, C. Takano, M.B. Mourão, and S.Y. Tagusagawa: IJBHT, 2013.
25. S.D. Dunmead and A.W. Weimer: US5756410 A, 1998.
26. H.M. Rietveld: *J. Appl. Crystallogr.*, 1969, vol. 2, pp. 65–71.
27. ASTM: Standard Test Method for Single Pellet Crush Strength of Formed Catalysts and Catalyst Carriers ASTM D4179-11, ASTM International, West Conshohocken, PA, 2011, http://www.astm.org.
28. L. Rongti, P. Wei, and M. Sano: *Metall. Mater. Trans. B*, 2003, vol. 34B, pp. 433–37.
29. W.B. Rogatz: US1422135, 1922.
30. L. Rongti, P. Wei, M. Sano, and J. Li: *Thermochim. Acta*, 2002, vol. 390, pp. 145–51.
31. R. Winand, M. Van Gysel, A. Fontana, L. Segers, and J.C. Carlier: *Trans Inst Min Metall (SectionC),* 1990, pp. 105–11.